Scanning Electron Microscopy Interpretation in Carbon Nanotubes Composite Materials after Postbuckling – Review Paper

Article · December 2014

CITATIONS
14

READS
917

3 authors:

Elias Randjbaran
48 PUBLICATIONS **407** CITATIONS
SEE PROFILE

Rizal Zahari
Military Technological College Oman (In partnership with the University of Portsm…
114 PUBLICATIONS **2,222** CITATIONS
SEE PROFILE

Ramin Vaghei
20 PUBLICATIONS **613** CITATIONS
SEE PROFILE

MATRIX ACADEMIC INTERNATIONAL ONLINE JOURNAL OF ENGINEERING AND TECHNOLOGY
ISSN: 2348-3326
© MAIOJET
OCTOBER 2014

Scanning Electron Microscopy Interpretation In Carbon Nanotubes Composite Materials After Postbuckling - Review Paper

Elias Randjbaran*, Rizal Zahari,Ramin Vaghei

Aerospace Manufacturing Research Centre (AMRC),Level 7, Tower Block, Faculty of Engineering, 43400 UPM Serdang ,Selangor - Malaysia.
** Corresponding author: Tel: +44 (0) 745 2203616, Fax: +44 (0) 844 7749975*
Elias@gmx.co.uk

***Abstract*—Current review paper summarizes the review on scanning probe microscopy investigations of the properties and manipulation of carbon nanotubes, and moreover, the fabrication and utilization of nanotubes as novel tips for probe microscopy experiments. For small aspect ratio nanotubes, the boundary constraints begin to play a major role in the post-buckling behavior and collapse need not be as catastrophic as in the longer structure. It is shown that the post-buckling deflection causes driving force mainly in the in-plane and out-of-plane shear modes and the bending mode about the wall length direction. Depending on the nature and magnitude of the interfacial toughness, the nano-wall may undergo no cracking, snap-back fracture and snap-through fracture.**

***Keywords*—Carbon Nanotubes, Scanning Electron Microscopy (SEM), Post-buckling**

I. INTRODUCTION

Carbon nanotubes are currently the focus of intense interest worldwide. This attention to carbon nanotubes is not surprising in light of their promise to exhibit unique physical properties that could impact broad areas of science and technology, ranging from super strong composites to nano-electronics [1, 2, and 3]. Recent experimental studies have shown that carbon nanotubes are the stiffest known material [4, 5] and buckle elastically (vs. fracture) under large bending or compressive strains [5&6, 20-34]. These mechanical characteristics suggest that nanotubes have significant potential for advanced composites, and could be unique force transducers to the molecular world. Moreover, the remarkable electronic properties of carbon nanotubes offer great intellectual challenges and the potential for novel applications [7-9].

It has been observed that unbuckling takes place at a different load than buckling. This is attributable to the fact that the ends of the fibrils detach from the compressing surface and lose adhesion to it during buckling and post-buckling. This phenomenon changes the boundary conditions on the end of the fibril and consequently modifies the load at which the fibril will unbuckle. Hui et al. [4, 20] developed a theoretical model for this process based on Euler–Bernoulli beam theory and linear elastic fracture mechanics, which allows the determination of the buckling and unbuckling loads dependent on the extent of detachment. We now extend this approach in order to predict load-displacement curves during buckling and unbuckling of a fibril. The resulting load-displacement curves give considerable insight into the buckling, post-buckling and unbuckling behavior of fibrils. Furthermore, the results suggest that effects of viscosity, inertia and friction may play an important role in the buckling and adhesion characteristics of fibrillar mats [21].

II. EXPRINCES

The mixing of the EP resin with the CNFs took place in a vacuum dissolver (Dispermat AE, VMA-Getzmann) in order to achieve a good dispersion of the fillers in the resin. The curing agent was added then and mixed by hand. Finally, the samples were cured in an oven using the same temperature profile for all of them. The final concentration of CNFs was 1 vol. %. The produced test specimens were examined by systematic scanning electron microscopic (SEM). In Figure 1a it is observed that a good level of uniformity and homogeneity is achieved in the EP/CNF mixture. Nevertheless, some rich-in-CNFs areas are visible

(marked by circles). The observation of these areas in larger magnification (Figure 1b) reveals that the CNFs are well wetted by the EP matrix and no pure CNF agglomerations are formed [10- 12].

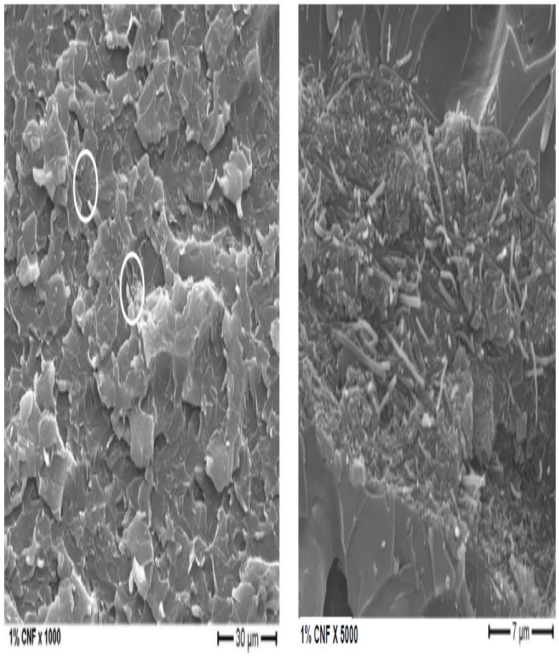

Fig. 1 SEM results of CNF-doped epoxy samples. A) x1000 magnification B) x5000 magnification of rich with CNFs area.

Tensile tests of dog-bone specimens were performed at a MTS 858 testing device with cross-head rate of 1 mm/min. The visco-elastic response of the various EP matrix samples was studied by dynamic mechanical thermal analysis (DMTA). An Eplexor TM 150N (Gabo Qualimeter) DMTA device was employed to carry out the tests. The specimens were subjected to oscillating dynamic loading consisting of a static preload of 4N on which a sinusoidal wave of 2 N at a constant frequency was superimposed. The measurements were made under tension loading with testing frequency of 10 Hz. Heating occurred at a rate of 2°C/min and in a temperature range between 20 to 150°C. The volume resistivity measurements were carried out by a resistivity meter (Hiresta UP, Mitsubishi Chemicals) [14-17].

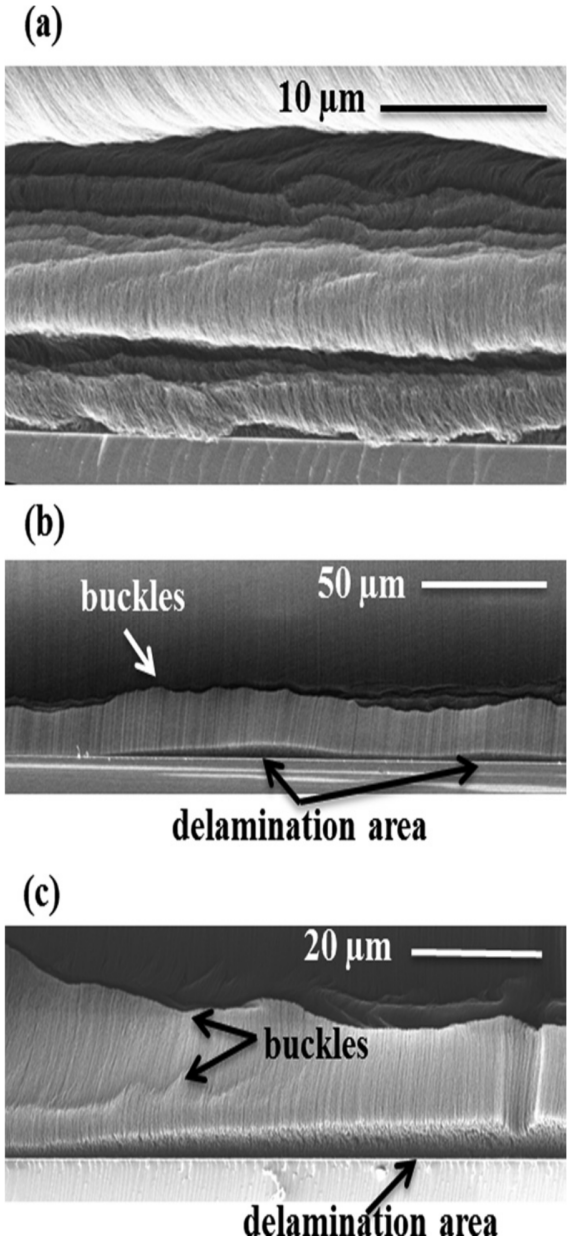

FIG. 2. SEM images of the CNT forests base, illustrating permanent deformation after macro-compression. (a) SEM image of an edge region with multiple buckles but no delamination. (b) SEM image of a location illustrating multiple buckles and delamination of CNTs. (c) A magnified view of a region where CNTs buckled and interface delamination occurred [18].

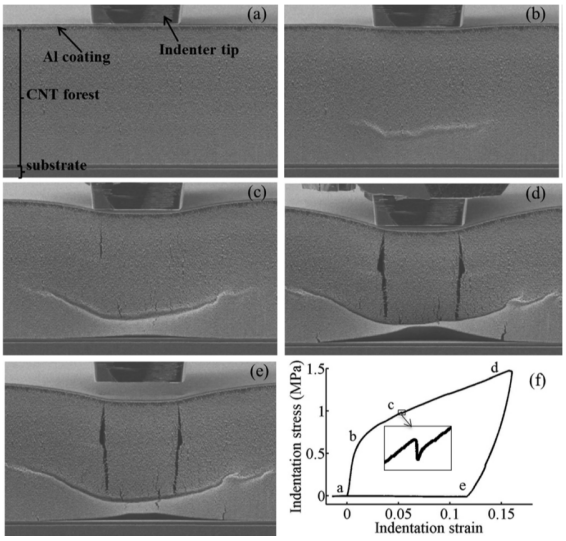

FIG. 3. SEM micrographs (a–e) and stress-strain data (f) illustrating the deformation of a CNT forest coated with a 1 lm Al film that was indented at its edge. Images correspond to points a–e on the indentation stress-strain curve in (f) [18].

II.I. SYNTHESIS OF THE COMPOSITE

The most important step is to synthesize this kind of composite. The idea is to grow carbon nanotubes on the piezoelectric ceramic discs (Fig. 4). The piezoelectric ceramic is to be used as a base.

The carbon nano particles are synthesized over the ceramic. These units are then cured in a suitable resin matrix to form a composite structure. The most viable resin matrix is epoxy. There are different grades of epoxy resin, but for experiment purpose the general purpose epoxy can be used, which is easily available in the market.

The growth of carbon nano fibers can be achieved using the techniques mentioned below:

– Laser ablation,
– Arc discharge,
– Chemical Vapor Deposition on a substrate,
– Chemical Vapor Deposition in an aerogel,
– Micro fabrication,
– Electros pining,
– Detonation of 2,4,6-triazido- 1,3,5-triazine in presence of transition metal.

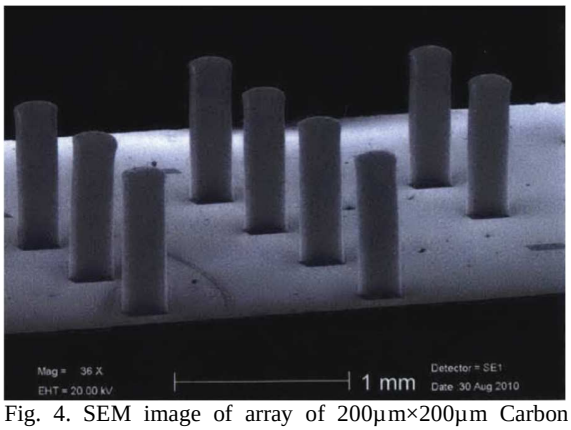

Fig. 4. SEM image of array of 200µm×200µm Carbon nanotube pillars

III. RESULTS AND DISCUSSION

III.I. EVOLVING POST-BUCKLING MORPHOLOGIES

A 20-walled CNT as a representative example to illustrate the deformation morphologies and energetics of thick MWCNTs under uniaxial compression. The aspect ratio of the MWCNT is $\rho = L / d = 5$, where L is the length, and d is the diameter of the outermost wall of the MWCNT (also regarded as the diameter of the MWCNT) [34].

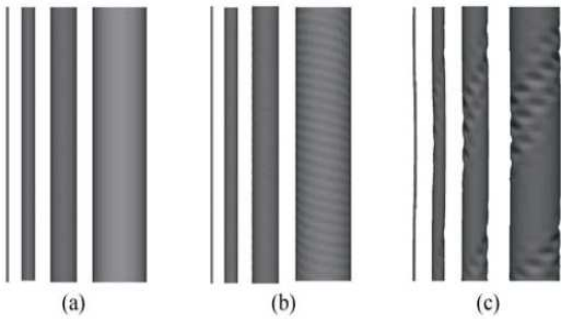

Figure 5 Evolution of the deformation morphologies of a uni-axially compressed 20-walled MWCNT. Each subfigure consists of four constituent shells of the 20-walled MWCNT. From left to right in each subfigure, the shells are the innermost, the 5th, the 10th, and the outermost shells. (a) Fully relaxed, un-deformed configuration. (b) At a compressive strain of $\varepsilon = 8.23\times10^{-3}$, wave-like ripples appear along the 10th and the outermost shells, while ripples are not observable in

the other two inner shells. (c) At a compressive strain of $\varepsilon = 1.18\times10^{-2}$, a helical diamond pattern runs from one end to the other for the outer three shells. The innermost shell is further bent and twisted throughout its length [34].

Figure 5 shows the deformation morphologies at different compressive strains. The deformation morphologies of four constituent shells—the innermost, the 5th, the 10th, and the outermost shells—are shown from left to right in each of Figs. 1(a)–1(c). We observed that, upon constraint-free geometry optimization as the first step (Fig. 1(a)), the shells in the MWCNT undergo rigid rotation with respect to their central axis. From innermost to outermost layers, the neighbouring shells rotate in alternating directions (clockwise and counter clockwise). We attribute this alternating rotation to the registry-dependent inter-shell interactions. In particular, the arrangement of the neighbouring shells in the initial configuration (the initial guess) is close to A–A stacking, which is energetically disfavoured. The rotations of the neighbouring shells in alternating [34].

Interestingly, after the buckling event (the system is now described as postbuckled), the force required to overcome the adhesion at the pinned end of the nanotube and enter the slip-stick domain is, by definition, the frictional force. A prediction can be made about the shape of the buckled nanotube as it undergoes further compression by applying an elastica model of a postbuckled column [23-30].

IV. CONCLUSIONS

The results show, first, the adhesion of long, straight, single-walled carbon nanotubes to surfaces is examined using multidimensional force spectroscopy. It has been observed characteristic signatures in the deflection and frequency response of the cantilever indicative of nanotube buckling and slip-stickmotion as a result of compression and subsequent adhesion and peeling of the nanotube from the surface. The spring constant and the elastic modulus of the SWNT were estimated from the frequency shifts under tension. Using elastica modelling for postbuckled columns, it has been concluded that the static coefficient of friction for the SWNT on alkanethiol-modified gold surfaces and showed that it varies with the identity of the monolayer terminal group. Therefore, without careful consideration of the spring constant of the AFM cantilever relative to the critical buckling load, high aspect ratio carbon nanotube AFM probes will buckle during imaging, even in intermittent contact mode.

References

1. Andersen, A. J., Robinson, J. T., Dai, H., Hunter, A. C., Andresen, T. L., & Moghimi, S. M. (2013). Single-walled carbon nanotube surface control of complement recognition and activation. ACS nano, 7(2), 1108-1119.

2. Duncan, R., & Gaspar, R. (2011). Nanomedicine (s) under the microscope. Molecular pharmaceutics, 8(6), 2101-2141.

3. Afkhami, A., Khoshsafar, H., Bagheri, H., & Madrakian, T. (2014). Facile simultaneous electrochemical determination of codeine and acetaminophen in pharmaceutical samples and biological fluids by graphene-CoFe2 O 4 nanocomposite modified carbon paste electrode. Sensors and Actuators B: Chemical.

4. Aykol, Mehmet, et al. "Clamping Instability and van der Waals Forces in Carbon Nanotube Mechanical Resonators." Nano letters (2014).

5. Rasmussen, Anna Julie, and Mette Ebbesen. "Characteristics, Properties and Ethical Issues of Carbon Nanotubes in Biomedical Applications." NanoEthics 8.1 (2014): 29-48.

6.Zhao, W., Li, Y., Wang, S., He, X., Shang, Y., Peng, Q., & Cao, A. (2014). Elastic improvement of carbon nanotube sponges by depositing amorphous carbon coating. Carbon, 76, 19-26.

7. Brieland-Shoultz, A., Tawfick, S., Park, S. J., Bedewy, M., Maschmann, M. R., Baur, J. W., & Hart, A. J. (2014). Scaling the Stiffness, Strength, and Toughness of Ceramic-Coated Nanotube Foams into the Structural Regime. Advanced Functional Materials.

8. Lee, J. I., Eun, Y., Choi, J., Kwon, D. S., & Kim, J. (2014). Using Confined Self-Adjusting Carbon Nanotube Arrays as High-Sensitivity Displacement Sensing Element. ACS applied materials & interfaces, 6(13), 10181-10187.

9. Harik, V. (2014). Trends in Recent Publications on Nanoscale Mechanics. In Trends in Nanoscale Mechanics (pp. 213-222). Springer Netherlands.

10. Tsantzalis, S., Tsotra, P., Karapappas, P., Vavouliotis, A., Fanis, N., Kostopoulos, V., & Friedrich, K. (2007). Influence of Carbon Nanofibers and Piezoelectric Particles on the Thermomechanical Behaviour of Epoxy Mixtures. Solid State Phenomena, 121, 1419-1424.

11. Kostopoulos, V., Tsotra, P., Karapappas, P., Tsantzalis, S., Vavouliotis, A., Loutas, T. H.,& Tanimoto, T. (2007). Mode I interlaminar fracture of CNF or/and PZT doped CFRPs via acoustic emission monitoring. Composites Science and technology, 67(5), 822-828.

12. TSANTZALIS, S., TSOTRA, P., KARAPAPPAS, P., VAVOULIOTIS, A., FANIS, N., KOSTOPOULOS, V., & FRIEDRICH, K. (2007). Influence of carbon nanofibers and piezoelectric particles on the thermomechanical behavior of epoxy mixtures. Diffusion and defect data. Solid state data. Part B, Solid state phenomena, 121, 1419-1422.

13.Kostopoulos, V., Tsotra, P., Vavouliotis, A., Karappapas, P., Tsantzalis, S., & Loutas, T. (2005, October). Nano-modified fiber reinforced composites: A way towards the development of new materials for space applications. In Proceedings of the Fifth ESA Symposium on Micro/Nano Technologies for Space.

14. Díez-Pascual, A. M., & Diez-Vicente, A. L. (2014). ZnO-reinforced Poly (3-hydroxybutyrate-co-3-hydroxyvalerate) Bionanocomposites with Antimicrobial Function for Food Packaging. ACS applied materials & interfaces.

15. Larsson, P. A., Berglund, L. A., & Wagberg, L. (2014). Ductile all-cellulose nanocomposite films fabricated from core-shell structured cellulose nanofibrils. Biomacromolecules.

16. He, Q., Yuan, T., Zhang, X., Luo, Z., Haldolaarachchige, N., Sun, L., & Guo, Z. (2013). Magnetically soft and hard polypropylene/cobalt nanocomposites: Role of maleic anhydride grafted polypropylene. Macromolecules, 46(6), 2357-2368.

17. Gong, Z., Gong, J., Yan, X., Gao, S., & Wang, B. (2011). Investigation of the effects of temperature and strain on the damping properties of polycarbonate/multiwalled carbon nanotube composites. The Journal of Physical Chemistry C, 115(38), 18468-18472.

18. Abadi, P. P. S. S., Hutchens, S. B., Greer, J. R., Cola, B. A., & Graham, S. (2013). Buckling-driven delamination of carbon nanotube forests. Applied Physics Letters, 102(22), 223103.

19. Huang, X., Yuan, H., Hsia, K. J., & Zhang, S. (2010). Coordinated buckling of thick multi-walled carbon nanotubes under uniaxial compression. Nano Research, 3(1), 32-42.

20. Hui, C.-Y., Jagota, A., Shen, L., Rajan, A., Glassmaker, N., & Tang, T., (2007). Design of Bio-Inspired Fibrillar Interfaces for Contact and Adhesion—Theory and Experiments, J. Adhes. Sci. Technol., 21, pp. 1259–1280.

21. Paretkar, D., Kamperman, M., Martina, D., Zhao, J., Creton, C., Lindner, A., ... & Arzt, E. (2013). Preload-responsive adhesion: effects of aspect ratio, tip shape and alignment. *Journal of The Royal Society Interface*, *10*(83), 20130171.

22. Barker, K. M., Poggi, M. A., Lizarraga, L., Lillehei, P. T., Ferri, A. A., & Bottomley, L. A. (2014). Peeling of long, straight carbon nanotubes from surfaces. *Journal of Nanotechnology*, *2014*.

23. Randjbaran, E., Zahari, R., Majid, D. L., Jalil, N. A. A., Vaghei, R., & Ahmadi, R. (2013) An Experimental Investigation of the Effects of Stacking Sequence on Hybrid Composite Materials Response to Open-Hole Compression Strength. MATRIX Academic International Online Journal of Engineering and Technology, 1(2), 1-6.

24. Randjbaran, E., Zahari, R., Majid, D. L., Jalil, N. A. A., Vaghei, R., & Ahmadi, R. (2013) The Effects of Stacking Sequence Layers of Hybrid Composite Materials in Energy Absorption under the High Velocity Ballistic Impact Conditions: An Experimental Investigation. MATRIX Academic International Online Journal of Engineering and Technology, 1(2), 30-37.

25. Randjbaran, E., Zahari, R., Majid, D. L., Jalil, N. A. A., & Vaghei, R. (2013) Effects of Stacking Sequence on Compression Response Testing of Carbon Fibre and Hybrids: Fibrous-Glass/Carbon/Kevlar/ Epoxy Composite Plates. MATRIX Academic International Online Journal of Engineering and Technology, 2(1), 13-17.

26. Randjbaran, E., Zahari, R., Majid, D. L., Jalil, N. A., Vaghei, R., & Ahmadi, R. (2013). The effects of stacking sequence layers of six layers composite materials in ballistic energy absorption. International Journal of Material Science Innovations, 1(6), 293-305.

27. Randjbaran, E., Zahari, R., Majid, D. L., Jalil, N. A. A., Vaghei, R., & Ahmadi, R. (2014). Experimental Study of the Influence of Stacking Order of the Fibrous Layers on Laminated Hybrid Composite Plates Subjected to Compression Loading. Journal of Science and Engineering, 4(1), 01-08.

28. Randjbaran, E., Zahari, R., Abdul Jalil, N. A., & Abang Abdul Majid, D. L. (2014). Hybrid Composite Laminates Reinforced with Kevlar/Carbon/Glass Woven Fabrics for Ballistic Impact Testing. The Scientific World Journal, doi:10.1155/2014/413753.

29. Karamizadeh, S., Abdullah, S. M., & Zamani, M. (2013). An Overview of Holistic Face Recognition. IJRCCT, 2(9), 738-741.

30. Karamizadeh, S., Abdullah, S. M., Manaf, A. A., Zamani, M., & Hooman, A. (2013). An Overview of Principal Component Analysis. Journal of Signal and Information Processing, 4, 173.

31. Karamizadeh, S., Abdullah, S. M., Zamani, M., & Kherikhah, A. (2014). PATTERN RECOGNITION TECHNIQUES: STUDIES ON APPROPRIATE CLASSIFICATIONS. Journal of Engineering & Applied Sciences, 9(8).

32. Karamizadeh, S., Shayan, J., Alizadeh, M., & Kheirkhah, A. (2013). Information Security Awareness Behavior: A Conceptual Model for Cloud. INTERNATIONAL JOURNAL OF COMPUTERS & TECHNOLOGY, 10(1), 1186-1191.

33. Karamizadeh, S., Abdullah, S. M., Halimi, M., Shayan, J., Rajabi, M. J. (2014) Advantage and Drawback of Support Vector Machine Functionality. IEEE 2014 International Conference on Computer, Communication, and Control Technology, I4CT 2014, 61-63.

34. Huang, X., Yuan, H., Hsia, K. J., & Zhang, S. (2010). Coordinated buckling of thick multi-walled carbon nanotubes under uniaxial compression. *Nano Research*, *3*(1), 32-42.